v. 4, n. 12, 2024

Journal of Engineering Research

ELIMINATION OF THE RASSF9 GENE IN THE B16F0 MELANOMA LINE THROUGH CRISPR/CAS9

Julia Souza e Costa

All content in this magazine is licensed under a Creative Commons Attribution License. Attribution-Non-Commercial-Non-Derivatives 4.0 International (CC BY-NC-ND 4.0).

Abstract: Melanoma is the cancer caused by the transformation of melanocytes, being the most lethal among skin cancers. It can be divided into four groups depending on the mutation present, with the most frequent changes in the B-Raf and Ras proteins. The Ras protein is associated with different signaling cascades, regulating processes such as proliferation, differentiation, morphology and apoptosis. The main effectors of Ras in cell death are members of the RASSF (Ras-association Family). RASSF9 has been implicated in keratinocyte differentiation and dermal homeostasis and, interestingly, its expression can be induced by sun exposure. To study the role of RASSF9 in melanomas, we will eliminate the expression of this gene in the B16F0 murine lineage, through the CRISPR/Cas9 system. After selecting a stable transfectant line (B16F0.R9KO), we will evaluate the impact of our manipulation on tumor growth in vitro and in vivo, as well as resistance to chemotherapy drugs. Finally, this lineage will serve as a tool for further studies on the role of RASSF9 in intracellular biochemical pathways and other aspects of tumor biology.

INITIAL CONSIDERATIONS

During the period from May to November 2022, we focused on culturing B16F0 cells, selecting the optimal antibiotic concentration, transforming competent bacteria, amplifying plasmids, transfecting HEK293T, producing the Lentivirus and transducing the lineage with LentiCRISPRv2 lentivirus carrying the validated sgRNA sequence for RASSF9. With no previous experience in the laboratory, the first months were essential for learning about and improving laboratory techniques.

In the following months, we carried out the extraction and worked on the use of nucleic acids, RNA extraction, cDNA synthesis, qPCR reaction, electrophoresis in agarose gel, labeling of specific proteins, obtaining protein extract, electrophoresis of proteins in Polyacrylamide gel (SDS Page), Western blot, growth assay and chemotherapy resistance assays.

ACADEMIC ACTIVITIES DURING THE SCHOLARSHIP PERIOD

Concomitantly with scientific initiation, I completed the 5th period of the medical course with an overall average of 9.6 and I am currently studying the 6th period at college, totaling 2462 hours in workload. To complement and experience the teachings provided by graduation, I took extension courses, became a member of the Academic Directory of the Medicine Course at Faculdade Anhembi Morumbi, occupying the position of Scientific Director, in addition to Scientific Director of the Infectious Diseases league, Assistant Editor of the Academic Medical Educational Magazine Anhembi Morumbi, Director of Neuroscience Extension - NGO Médicos do Mundo, member of the Instituto da Memória and Scientific Director of the League of Infectious Diseases (LAI-UAM) in addition to being an active member of the Academic League of Oncogenetics – Hospital A.C. Camargo Cancer Center, Infectious Diseases – UAM and started an internship at Hospitals Israelita Albert Einstein - Morumbi, Reference Center for Inborn Errors of Metabolism – Unifesp, Military Police Hospital of the State of São Paulo and Berrini Medical Center. Furthermore, I participated in the São Paulo Congress of Infectious Diseases, where I took courses on Arboviruses and Infection in immunosuppressed patients, as well as being present at the V EVA National Symposium on Gynecological Oncology, Alzheimer's Association International Conference (2022), Workshop on a Humanized Approach to Dementia and Simulation of first aid for neurological

trauma, among other events (Figure 1). I wrote the chapter "The role of genetic markers in the treatment of meningiomas" for the book "Oncology and Hematology – Edition II" (https://doi.org/10.29327/584510.2-3), and other articles, such as "Letter: Importance of Cobalt-60 Dose Rate and Biologically Effective Dose on Local Control for Intracranial Meningiomas Treated With Stereotactic Radiosurgery" recently published in the journal Neurosurgery (doi: 10.1227/neu.0000000000002137), "Case Report – Facial Nerve Palsy associated with COVID-19 infection", case report that I presented orally at the 7th Edition of International Conference on Neurology and Brain Disorders (INBC 2022). In addition to these works cited in the initial report, I participated in the production of the review article "Resection of low grade temporal gliomas and the improvement of convulsive seizures" which was selected for presentation in the poster session during the XIV São Paulo Congress of Neurology, as we also wrote a letter to the editor "Letter to the editor: late recovery of stereotactic radiosurgery induced perilesional edema of an arteriovenous malformation after Bevacizumab treatment" published in the British Journal of Neurosurgery (https://doi.org/10.1080/02688697.2023.2228890).

Given the above, I celebrate the achievements of the last few months and conclude that they were due to the opportunity to experience science in Prof. Dr. João Gustavo Pessini Amarante-Mendes, providing me with enriching teachings, satisfaction and respect for research.

METHODOLOGY

CELL LINEAGE

Cells from the B16F0 murine melanoma line were cultured in 10% RPMI medium and HEK293T human embryo kidneys. The first was grown in 10% RPMI medium, while HEK293T was grown in 10% DMEM.

CULTURE MEDIUM

We cultured the cells in RPMI-1640 media (Thermo Fisher), supplemented with 10% fetal bovine serum (Thermo Fisher), 1% L-Glutamine (Thermo Fisher) and 1% of the antibiotics penicillin and streptomycin (Thermo Fisher); DMEM (Thermo Fisher), supplemented with 10% fetal bovine serum (Thermo Fisher), 2mM L-Glutamine (Thermo Fisher) and 100 µg/ml of the antibiotics penicillin and streptomycin (Thermo Fisher); UNDER (2% Bacto-tryptone, 0.5% yeast-extract, 10mM NaCl, 2.5mM KCl, 10mM MgCl2, 10mM Mg2SO4, H2O milli-Q qsp 600mL, adjusting the pH to 7.0); SOB agar (100mL of SOB after increasing the pH and adding 1.5g of Bacto Agar); Luria-Bertani ([LB] Kasvi); LB agar (Kasvi).

PREPARATION OF DH5A SUPERCOMPETENT BACTERIA

We produced DH5a supercompetent bacteria using the Inoue method. We plated the bacteria on previously prepared SOB agar medium and incubated overnight at 37ºC for growth to occur. The following day, we selected an isolated colony and transferred it to an Erlenmeyer flask containing 10ml of sterile SOB medium (pre-inoculum), incubating the flask under shaking overnight (37ºC, 300rpm). The bacteria must grow with an optical density of 400-600nm. To do this, we wait 18 hours and insert 3ml of this solution into a sterile Erlenmeyer flask

Figure 1. Certificates of activities carried out from May to November with workload (C.H.). A, IV Inspirali Individual Progress Test (IPT). B, Extension Course "Mind in action: Meditation and Science" (C.H. 30h). C, Access to COVID-19 content: late complications – Instituto Israelita de Ensino e Pesquisa Albert Einstein (C.H. 1.3h). D, V EVA National Symposium on Gynecological Oncology (C.H. 12h). E, Certificate of oral presentation at the "6th Edition of International Conference on Neurology and Brain Disorders" held on October 24-26, 2022 in Orlando, Florida, USA. F, Arbovirus Course (C.H. 4h). G, Course of infection in immunosuppressed patients (C.H. 4h). H, 13th Paulista Congress of Infectious Diseases (C.H. 24h). I, Arbovirus Course (C.H. 4h). J, Neurology Congress (C.H. 40h). L, Workshop on a humanized approach to dementia and simulation of first aid for neurological trauma (C.H. 4h). M, Neurological Diseases Course (C.H. 40h). N, Alzheimer's Association International Conference (C.H. 40h). O, Poster Presentation and participation in the IX Academic Congress of Neurosciences - CAN (C.H. 3pm). P, Publication of a Chapter in the book Oncology and Hematology – Edition II.

containing 50ml of SOB medium (inoculum) and incubate for 1 hour under shaking (150rpm). We measured the absorbance on a spectrophotometer and when the OD 600 value was reached, the 50ml of inoculum was transferred to a falcon tube, incubated for 10 minutes on ice and centrifuged (3200g for 15 minutes at 4ºC). We resuspended the pellet with 20 ml of sterile ITB buffer and incubated it on ice for 10 minutes, repeating the centrifugation and gently resuspending the pellet with 4 ml of ITB buffer. We added 280ul of DMSO and incubated in a falcon tube on ice for 10 minutes. Once the bacteria were homogenized, we dispensed them in 100ul aliquots into eppendorf tubes and quickly submerged them in a container containing liquid nitrogen to promote rapid freezing.

AMPLIFICATION OF LENTICRISPRV2 PLASMIDS

We used the bacteria prepared for amplification of the empty vector LentiCRISPRv2 plasmids containing the genes for resistance to ampicillin, for the selection of bacteria, and to puromycin, to select mammalian cells, as well as the lentiRASSF9 plasmid, containing the sequences described previously, and also the gene responsible for encoding the Cas9 protein, fused to the Flag epitope. To do this, we transformed Sbl3 bacteria using the heat shock method. We added the plasmids to the bacteria and incubated them on ice for 30 minutes, then 2 minutes at 42ºC, and finally, we repeated the 2 minutes on ice. We added 1mL of LB medium to the tube, which was shaken for one hour (37ºC). After this period, we

inoculated the transformed bacteria in a petri dish containing 1.5% LB-agar medium with 100µg/ml ampicillin and incubated at 37ºC for 18 hours. We plated the bacteria in liquid medium to extract plasmid DNA.

PRODUCTION OF LENTIVIRAL PARTICLES

Lentiviral particles derived from the empty vector and the vector containing RASSF9 sgRNA were produced in 293T cells. For the production of lentiviruses, HEK 293T cells were previously maintained in 10% DMEM culture medium for a few days before starting the protocol. The day before transfection, 2x105 HEK293T cells were plated per well in a 6-well plate. After approximately 24 hours, confluence of approximately 80% was confirmed for transfection. For transfection, we incubated 1 ml of a solution containing 5µg of the empty vector (LentiCRISPR. v2) or cloned with the RASSF9 sgRNA (LentiCRISPR.sgRNA.R9), 3.5µg of the helper packaging plasmid (pCMV-VSV-G), 2.5 µg of envelope plasmid (psPAX-2), 22.5 µl of 1mg/mL Polyethylenimine (PEI) and topped up with serum-free DMEM to adjust the volume to 1 mL. As a transfection control, HEK 293T cells did not receive the LentiCRISPR. v2 plasmid. The following day, the culture medium was carefully changed to collect the viral supernatant 24 hours after this change.

TRANSDUCTION OF B16F0 CELLS WITH VIRAL SUPERNATANT

To carry out the transduction step, we used two 6-well plates, one of which was used as a control. 2x105 B16F0 cells were plated in each of these 12 wells with 2ml of RPMI10%. The following day, we removed 1500µl of medium from each well and incubated 1000µl of the collected supernatants (one plate for the solution with Lenti CRISPR. v2 empty vector and the other for the solution with LentiRASSF9) in the presence of Polybrene (5µg/ml - Sigma-Aldrich), at 37ºC, 5% CO2. After 48 hours, Puromycin (Invitrogen) was added to select transfected cells. For the next 7 days, the cells were maintained in the presence of puromycin and subcultured whenever necessary.

EXTRACTION AND USE OF NUCLEIC ACIDS

RNA EXTRACTION

We washed the B16F0, B16F0.EV and B16F0.R9KO cell lines with 1X PBS, deadhered with trypsin, collected and centrifuged for 5 minutes at 500 x g. We resuspended the formed pellet in culture medium, counted the cells and separated 1x106 cells. We centrifuged at 500 x g and resuspended the pellet in 500 µL of TRIzolTM reagent (TermoFisher). We freeze this solution in a -80°C freezer.

To perform the extraction, we thawed the frozen samples on ice and added 100 µL of chloroform. We homogenized the samples and maintained at room temperature for 3 minutes. After this time, we centrifuged the samples at 12,000 x g at 4°C for 15 minutes.

At this stage, we obtained 3 phases, the upper phase being the one in which the RNA is present. We collected the upper phase and added 250 µL of isopropanol. We vortexed the samples and kept them at room temperature for 15 minutes. We then centrifuged at 12,000 x g for 15 minutes at 4°C. We discarded the supernatant, added 500 µL of ice-cold 75% ethanol to the pellet, and centrifuged at 7500 x g for 5 minutes at 4°C. We repeated the step with ethanol two more times, removed the excess ethanol and waited for the ethanol to completely evaporate. We added 20 µL of H2O DNAse free/RNAse free to the samples and incubated at 60°C for 10 minutes. After 10 minutes, we quickly placed the samples on ice and quantified them using the Nanodrop 2000 (TermoFisher).

SYNTHESIS OF CDNA

We use the extracted RNA for cDNA synthesis following the steps in topic 3.7.1. We used the enzyme ImProm-IITM Rever Trancripase (Promega) following the manufacturer's recommendations. Into the 10 µL total volume solution, we added 2 µg of RNA and 0.5 µg of oligo(dT) 12-18 (TermoFisher). We incubated the samples at 70°C for 5 minutes and then for another 5 minutes on ice. We added 1X volume of the ImProm-II reaction buffer, 3mM of MgCl2, 0.5mM of each dNTP and 1µL of the ImProm-IITM Reverse Transcriptase enzyme to this solution. We incubated the solution with a final volume of 20 µL for 1 hour at 42°C and continued with inactivation of the enzyme by incubation at 70°C for 15 minutes. We store the product at -20°C until it is used in qPCR.

REACTION OF QPCR

We applied the qPCR reaction to determine the expression level of the RASSF9 and b-actin genes. To the reaction mixture, we added 5µl of SYBR Green PCR Master Mix (TermoFisher), 100ng of cDNA, and the standardized concentration of each primer pair. We adjusted the volume with H2O DNAse free/RNAse free to 10 µL. In amplification, we used the threshold cycle (CT) values of each sample, acquired in the exponential phase of the reaction for the 2-ΔΔCt calculations. We regularized the values by β-actin housekeeping.

AGAROSE GEL ELECTROPHORESIS

To perform electrophoresis in agarose gel (1% and 2%) as described by Sambook and Russel (J. SAMBROOL, D.W. RUSSEL, 2001), we dissolved the agarose in TAE and submerged the gel in the same buffer. Then, a potential difference (70V to 100V) was applied under constant amperage. We stained the molecules with 0.5 µL ethidium bromide for 20 minutes and visualized them on a transilluminator with UV light (260 nm).

TAGGING SPECIFIC PROTEINS

OBTAINING PROTEIN EXTRACT

We washed 106 cell units using 1X buffered saline solution (PBS), twice, with centrifugation for 5 minutes at 5000 x g. Next, we added a sample buffer for 1X proteins to the collected material and subjected it to a 5-minute incubation at 95°C. The product was stored at a temperature of -20°C until handling.

POLYACRYLAMIDE GEL ELECTROPHORESIS OF PROTEINS (SDS PAGE)

We inserted the samples, accompanied by the BenchMarck Ladder protein molecular mass marker (Invitrogen) into a denaturing polyacrylamide gel containing appropriate solutions and concentrations. Then, we subsequently subjected the gels to the Western blotting technique.

WESTERN BLOT

To analyze the expression of specific proteins using antibodies, we transferred the proteins to a nitrocellulose membrane (Amersham HybondTM-C, GE Healthcare) after performing electrophoresis in a polyacrylamide gel. We performed the transfer using a specific buffer in a SemiDry system (BioRad), with 30 V for 30 minutes.

We stained the membrane with 0.1% Ponceau S in 1% acetic acid after performing the transfer. We performed the blocking using 5% whole milk in PBS 0.1% Tween 20, with constant stirring for 1 hour at room temperature. We added the primary antibody and incubated at room temperature with gentle shaking. The antibodies used in this process were RASSF9 Polyclonal

Antibody (Invitrogen) 1:500 and β-actin (8H10D10) mouse mAb #3700 (Cell Signaling Technology) 1:1000, in the informed dilutions. After incubation, the membrane was washed three times with PBS/0.1% Tween 20, and then incubation with mouse (1:1000) and rabbit (1:1000) α-IgG secondary antibodies. conjugated with HRP, both diluted in 5% milk solution in PBS 0.1% Tween 20 for 1 hour, with constant stirring. We performed washes after incubation with the secondary antibody and revelation was performed with homemade ECL using the ImageQuantTM LAS 4000 equipment (GE Healthcare Life Sciences).

GROWTH ASSAY

To evaluate the proliferative capacity of the knockout line obtained, a growth curve will be performed, plating 1 x 104 cells per well of 6-well plates. After 24, 48, 72, 96, 120 and 144 hours, the cells will be isolated, stained with 0.2% trypan blue and counted using the Countess II automatic counter (Thermo Fisher).

CHEMOTHERAPY DRUG RESISTANCE TRIALS

To evaluate the effect of the absence of RASSF9 in B16F0 cells on resistance to apoptosis, B16F0 and B16F0.R9KO cells will be incubated with different concentrations of staurosporine and the induction of apoptosis will be evaluated by labeling with 2µg/ml of Annexin V conjugated with Alexa Fluor 647 and 50nM of Sytox Green (Thermo Ficher), using the flow cytometry technique (BD FACSCanto™ II). Data will be analyzed using FlowJo v10 software.

RESULTS

CELL CULTIVATION

As the most fundamental technique used in our project, my training began with the practice of cell cultivation. B16-F0 cells were thawed, grown, and frozen until I became proficient. In Figure 2, different stages of the process are represented, from the moment they were trypsinized (Figure 2A), until they reached confluence at different magnifications (Figure 2B-D)

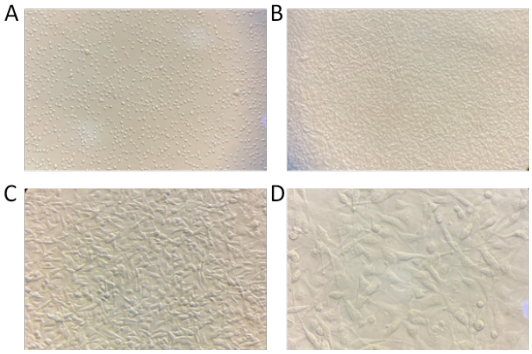

Figure 2. Representative image of cultures plating 1x105 B16F0 cells in RPMI10% FCS medium. A, 1x105 B16F0 cells/ml immediately after being trypsinized at 0.5x magnification. B, 5x106 B16F0 cells/ml four days after being trypsinized at 0.5x magnification. C, 5x106 B16F0 cells/ml four days after being trypsinized at 10x magnification. D, 5x106 B16F0 cells/ml four days after being trypsinized at magnification 20x.

ESTABLISHMENT OF PUROMYCIN CONCENTRATION FOR SELECTION OF TRANSDUCED CELLS

Before starting the transduction of B16-F0 cells, we established the ideal concentration of puromycin to be used in the selection of transduced cells. For this, 1x105 cells were plated in 6-well plates and after 24h, different concentrations of the antibiotic (0.6-1.4µg/ml) were added to the respective wells. In addition to the concentrations tested (Figure

3. A-E), B16F0 were plated on the same day, but without the presence of antibiotic to use as control (Figure 3.F). The concentration of 1.2 µg/ml of puromycin was chosen because it was the concentration at which 90%-95% of the cells died in 3 to 5 days.

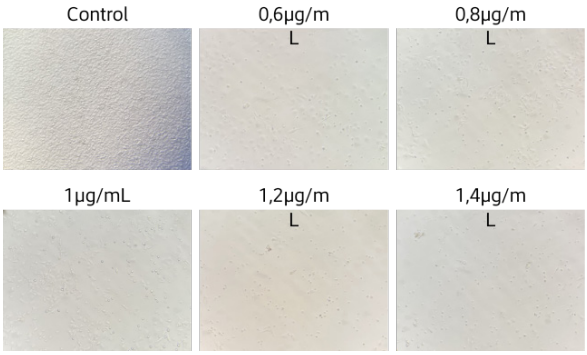

Figure 3. Optimization of puromycin concentration. Representative image of the treatment of B16-F0 cells treated with different concentrations of puromycin for the selection of transduced cells.

TRANSFECTION OF HEK293T CELLS

To carry out the transfection of HEK293T cells, 1.5 x 106 cells were plated in two 10cm dishes. Plasmid concentrations were measured using a nanodrop 2000, and then the necessary amounts of each plasmid were mixed with PEI to form the complex. We slowly dripped the contents onto the HEK293T cells and incubated them at 37ºC. After 24h, the culture medium was replaced and after another 24 hours, the supernatant containing the viral content was collected (Figure 4).

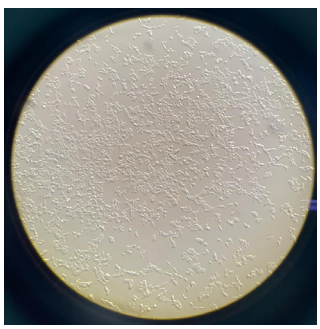

Figure 4. Representative image of transfected HEK293T cell cultures at 10x magnification.

TRANSDUCTION OF B16-F0 CELLS

To obtain cells containing the empty vector (B16F0.EV) and RASSF9 knockout cells (B16-F0.R9KO), the respective viral supernatants obtained in the transfection step were added to the B16-F0 cells. After 24 hours, the cells were treated with the selection antibiotic, putomycin (1.2µg/mL), for two weeks. The resistant cells were grown, frozen and then proceeded with their characterization (Figure 5).

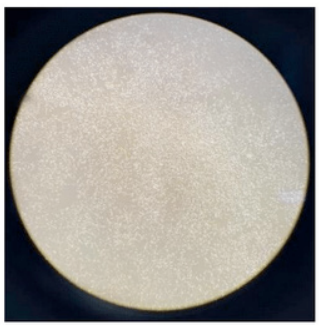

Figure 5. Representative image of B16-F0 lentivazio cells in 1.2 µg/ml puromycin concentration 6 days after transduction.

RASSF9 GENE EXPRESSION LEVELS BY QPCR

To characterize the B16-F0, vector and knockout lines, initially the expression levels of RASSF9 were measured at the RNA level by qPCR (Figure 6). We expected to obtain a higher expression level in the B16F0 lineage, similar to the level in B16F0.EV (vector) and reduced in B16F0.R9KO. However, the result did not occur as planned, possibly due to changing samples as many samples were prepared at the same time. Due to the inconsistency of results, we repeated the experiments to confirm the results found in the lines B16F0, B16F0.Vec, B16F0.R9KO, Tm5, Tm5.Vec and Tm5.R9KO (Figure 7). We expected that the expression of B16F0 would be similar to the expression of B16F0.Vec but they continued to express less. We will repeat the experiments to confirm the results.

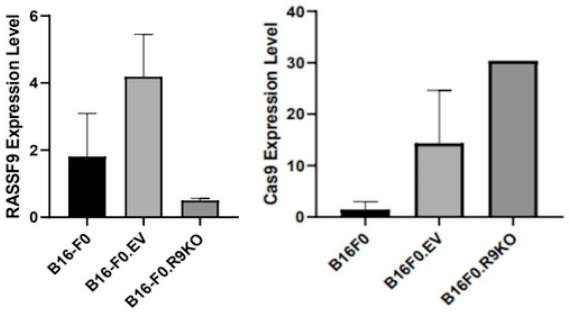

Figure 6. RASSF9 expression in B16-F0 murine melanoma. Assessment of the relative expression of RASSF9 at the mRNA level by qPCR in the B16F0, B16F0.EV and B16F0. R9KO lines.

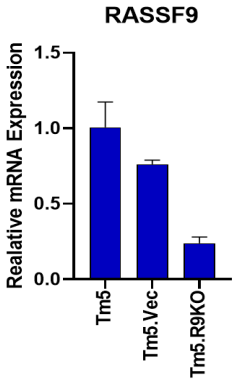

Figure 7. RASSF9 expression in Tm5 murine melanoma cell line. Assessment of the relative expression of RASSF9 at the mRNA level by qPCR in the Tm5, Tm5.Vec and Tm5.R9KO lines.

ASSESSMENT OF RASSF9 DEPLETION BY WESTERN BLOT

Continuing with the characterization of B16-F0 and Tm5 cells, we carried out protein evaluation of RASSF9 and Cas9. In both lines, Cas9 expression was significantly elevated in both vector cells and RASSF9 knockout cells (Figure 8 and 9). However, in the original cells, Cas9 expression was non-existent. Regarding RASSF9 expression, we noticed a reduction in Tm5 cells, although it was not completely eliminated. This may indicate the presence of a homogeneous population. Clones of these cells were generated and are in the process of characterization. As for B16-F0 cells, we did not detect any signal for RASSF9. Therefore, it will be necessary to repeat the Western Blot to finalize the characterization of these cells.

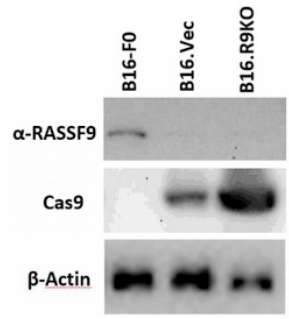

Figure 8. Assessment of RASSF9 depletion in B16-F0 cells by Western Blot

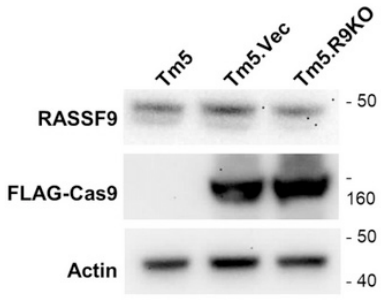

Figure 9. Assessment of RASSF9 depletion in TM5 cells by Western Blot

2.7 Growth test of the lines under study

The proliferative capacity of B16F0, B16F0.Vector and B16F0.R9KO cell lines, 1 x 104 cells were plated in 6-well plates and counted after 24, 48, 72, 96, 120 and 144 hours using 0.2% trypan blue and the Countess II automatic counter (Thermo Fisher). The results demonstrated differences in cell growth between B16-F0 cells on day 6 (Figure 10).

The B16F0 lineage recorded a total of 146.3 cells, while the B16F0.Vector lineage showed 157.3 cells (Figure 11). On the other hand, the B16F0.R9KO line exhibited a reduction in the number of cells, 76.97 cells counted. These results indicate that RASSF9 knockout cells have reduced proliferative capacity.

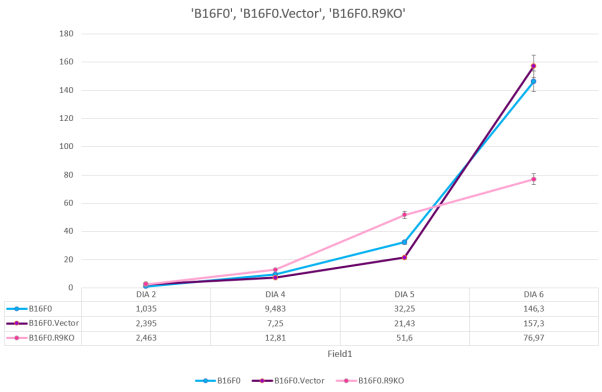

Figure 10. Growth curve of Lineages B16F0, B16F0.Vector and B16F0.R9KO

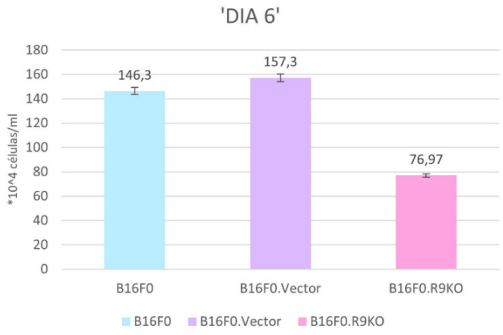

Figure 11. Growth of Lineages B16F0, B16F0. Vector and B16F0.R9KO on Day 6

DEATH RESISTANCE TEST WITH STAUROSPORINE

The ability to resist cell death was assessed by the percentage of cells positive for Annexin-V, which binds to phosphatidylserine that are exposed at the beginning of the apoptosis process, and Sytox Green, a fluorescent nucleic acid marker that does not cross cell membranes. viable cells, but easily marks the genetic material of cells in the process of cell death.

Thus, B16-F0 and Tm5 cells were treated with 1μM staurosporine for 24 hours and then labeled with Annexin-V and Sytox Green (Figure 12). The results show possible resistance to staurosporine treatment in Tm5. R9KO cells. These cells showed greater cell viability compared to the original cells and the vector cells. On the other hand, in B16-F0 cells, we observed a difference between the treated groups. To confirm these results, further tests with other drugs will be necessary, as well as the completion of the characterization of RASSF9 knockout cells.

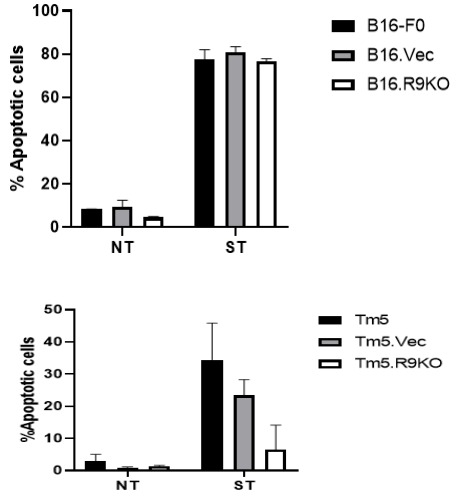

Figure 12. Induction of apoptosis by staurosporine. Representative graph of B16-F0 and Tm5 cells after treatment with staurosporine (1μM).

CONCLUSION

Although full characterization of B16-F0 and Tm5 cells has not been achieved, our preliminary results suggest a decrease in RASSF9 levels. This decrease, although not total, appears to have impacted the rate of cell proliferation. However, interestingly, this reduction in RASSF9 levels does not appear to influence cell resistance to staurosporine-induced death. It is important to highlight that these results are still preliminary and not conclusive. Therefore, further experiments will be needed to confirm these observations and fully elucidate the role of RASSF9 in cell proliferation and survival.

REFERENCES

AKBANI, R. et al. Genomic Classification of Cutaneous Melanoma. **Cell**, v. 161, n. 7, p. 1681–1696, 2015.

ALBERTS, B. et al. **Molecular Biology of the Cell** 6e. [s.l: s.n.]. v. 6, 2014

ASCIERTO, P. A. et al. The role of BRAF V600 mutation in melanoma**. Journal of translational medicine**, v. 10, p. 85, 2012.

AZOURY, S. C.; LANGE, J. R. **Epidemiology, Risk Factors, Prevention, and Early Detection of MelanomaSurgical Clinics of North America**, 2014.

BALCH, C. M. et al. Final version of 2009 AJCC melanoma staging and classification. **Journal of Clinical Oncology**, 2009.

BITRA, A. et al. Rassf proteins as modulators of Mst1 kinase activity. **Scientific Reports**, v. 7, n. February, p. 1–11, 2017.

BULMAN, A.; NEAGU, M.; CONSTANTIN, C. Immunomics in Skin Cancer - Improvement in Diagnosis, Prognosis and Therapy Monitoring. **Current Proteomics**, 2013.

CHEN, L.; JOHNSON, R. C.; MILGRAM, S. L. P-CIP1, a novel protein that interacts with the cytosolic domain of peptidylglycine ??-amidating monooxygenase, is associated with endosomes. **Journal of Biological Chemistry**, v. 273, n. 50, p. 33524–33532, 1998.

CHUMMUN, S.; MCLEAN, N. R**. The management of malignant skin cancersSurgery (United Kingdom)**, 2017.

COX, A. D.; DER, C. J. Ras history. **Small GTPases**, v. 1, n. 1, p. 2–27, 2010.

Dhanaraman T, Singh S, Killoran RC, et al. RASSF effectors couple diverse RAS subfamily GTPases to the Hippo pathway. ***Sci Signal***, 2020

GALLUZZI, L. et al. Molecular mechanisms of cisplatin resistance. **Oncogene**, v. 31, n. 15, p. 1869–1883, 2012.

GOLDSTEIN, B. G.; GOLDSTEIN, A. O. **Diagnosis and management of malignant melanoma American Family Physician**, 2001.

GUY, J. B. et al. Evaluation of the cell invasion and migration process: A comparison of the video microscope-based scratch wound assay and the boyden chamber assay. Journal of Visualized Experiments, v. 2017, n. 129, p. 56337, 2017.

HAURI, S. et al. Interaction proteome of human Hippo signaling: Modular control of the co-activator YAP1. **Molecular Systems Biology**, v. 9, n. 1, p. 1–16, 2013.

HENNIG, A. et al. Ras activation revisited: Role of GEF and GAP systems. **Biological Chemistry**, v. 396, n. 8, p. 831–848, 2015.

HUTCHINSON, F.; CANCER, S.; ALLIANCE, C. Treatment of Metastatic Melanoma : An Overview - Cancer Network Treatment of Metastatic Melanoma : An Overview Treatment of Metastatic Melanoma : An Overview - Cancer Network. **Network**, v. 23, n. 6, p. 1–7, 2010.

IGLESIAS GÃ3MEZ, J. C.; MOSQUERA ORGUEIRA, A. An Integrative Analysis of Meningioma Tumors Reveals the Determinant Genes and Pathways of Malignant Transformation. **Frontiers in Oncology**, v. 4, n. June, p. 1–12, 2014.

JIANG, C. et al. Application of CRISPR/Cas9 gene editing technique in the study of cancer treatmentClinical Genetics. **Blackwell Publishing** Ltd, 2020.

KITA, R.; FRASER, H. B. Local Adaptation of Sun-Exposure-Dependent Gene Expression Regulation in Human Skin. **PLoS Genetics**, v. 12, n. 10, p. 1–18, 2016.

LEE, C. M. et al. A novel role of RASSF9 in maintaining epidermal homeostasis. **PLoS ONE**, v. 6, n. 3, 2011.

LEE, SH., Meng, X., Flatten, K. *et al.* Phosphatidylserine exposure during apoptosis reflects bidirectional trafficking between plasma membrane and cytoplasm. *Cell Death Differ* **20,** 64–76, 2013.

LI, B. et al. MicroRNA-1254 exerts oncogenic effects by directly targeting RASSF9 in human breast cancer. **International Journal of Oncology**, v. 53, n. 5, p. 2145–2156, 2018.

LI, W.; MELTON, D. W. Cisplatin regulates the MAPK kinase pathway to induce increased expression of DNA repair gene ERCC1 and increase melanoma chemoresistance. **Oncogene**, v. 31, n. 19, p. 2412–2422, 2012.

MANUSCRIPT, A. NIH Public Access. v. 11, n. 11, p. 761–774, 2013.

MERLINO, G. et al. The state of melanoma: challenges and opportunities. **Pigment Cell and Melanoma Research**, v. 29, n. 4, p. 404–416, 2016.

MILLER, R. P. et al. **Mechanisms of cisplatin nephrotoxicity Toxins**, 2010.

RAN, F. A. et al. Genome engineering using the CRISPR-Cas9 system. **Nature Protocols**, v. 8, n. 11, p. 2281–2308, 2013.

RIEDL, A. et al. Comparison of cancer cells in 2D vs 3D culture reveals differences in AKT–mTOR–S6K signaling and drug responses. **Journal of Cell Science**, v. 130, n. 1, p. 203–218, 2017.

SÁNCHEZ-SANZ, G. et al. MST2-RASSF protein-protein interactions through SARAH domains. **Briefings in Bioinformatics**, v. 17, n. 4, p. 593–602, 2016.

SÁNCHEZ-TOMÉ, E. et al. Genome-wide linkage analysis and tumoral characterization reveal heterogeneity in familial colorectal cancer type X. **Journal of Gastroenterology**, v. 50, n. 6, p. 657–666, 2015.

SCHADENDORF, D. et al. Melanoma. **Nature Reviews Disease Primers**, n. April, p. 15003, 2015.

SCHADENDORF, D.; KOCHS, C.; LIVINGSTONE, E. Handbook of 96 Cutaneous Melanoma. p. 13–28, 2013.

SHALEM, O. et al. Genome-Scale CRISPR-Cas9 Knockout Screening in Human Cells. **Science**, v. 343, n. 6166, p. 84–87, 2014.

SHERWOOD, V. et al. RASSF7 Is a Member of a New Family of RAS Association Domain – containing Proteins and Is Required for Completing Mitosis. v. 19, n. April, p. 1772–1782, 2008.

Shi H, Ju Q, Mao Y, et al. TAK1 Phosphorylates RASSF9 and Inhibits Esophageal Squamous Tumor Cell Proliferation by Targeting the RAS/MEK/ERK Axis. **Adv Sci (Weinh)**. 2021

SIEGEL, R. L.; MILLER, K. D.; JEMAL, A. Cancer statistics, 2017. **CA: A Cancer Journal for Clinicians**, v. 67, n. 1, p. 7–30, 2017.

TSAO, H. et al. Early detection of melanoma: Reviewing the ABCDEs American Academy of Dermatology Ad Hoc Task Force for the ABCDEs of Melanoma. **Journal of the American Academy of Dermatology**, v. 72, n. 4, p. 717–723, 2015.

VAVVAS, D. et al. Identification of Nore1 as a potential Ras effector. **Journal of Biological Chemistry**, v. 273, n. 10, p. 5439–5442, 1998.

VORA, N. Melanoma and BRAF. v. 600, p. 6–9, 2014.

Yuan, J., Ju, Q., Zhu, J. *et al.* RASSF9 promotes NSCLC cell proliferation by activating the MEK/ERK axis. *Cell Death Discov.* **7,** 199 (2021).

ZHENG, X. et al. The coiled-coil domain of oncogene RASSF 7 inhibits hippo signaling and promotes non-small cell lung cancer. v. 8, n. 45, p. 78734– 78748, 2017.

ZHANG, P. et al. ASPP1 / 2-PP1 complexes are required for chromosome segregation and kinetochore-microtubule attachments. v. 6, n. 39, [s.d.].